IEEE Access
Multidisciplinary | Rapid Review | Open Access Journal

Received 23 January 2024, accepted 5 February 2024, date of publication 8 February 2024, date of current version 14 February 2024.

Digital Object Identifier 10.1109/ACCESS.2024.3363898

RESEARCH ARTICLE

Dual Mode PID Controller for Path Planning of Encoder Less Mobile Robots in Warehouse Environment

R. KARTHIK[1], R. MENAKA[1], P. KISHORE[2], R. ASWIN[2], AND CHARAN VIKRAM[2]
[1]Centre for Cyber Physical Systems (CCPS), Vellore Institute of Technology, Chennai 600127, India
[2]School of Electronics Engineering, Vellore Institute of Technology, Chennai 600127, India

Corresponding author: R. Menaka (menaka.r@vit.ac.in)

ABSTRACT Mobile robots have emerged as versatile substitutes for human labor across diverse domains, offering promising applications in surveillance, healthcare, and beyond. Fundamental to their autonomy are the core capabilities of movement, perception, cognition, and navigation. This research introduces a novel approach known as the Dual PID based low-cost navigation system (DPLNS), designed specifically for indoor warehouse-like environments. The primary objective of this technique is to enable seamless point-to-point traversal. This is achieved through a fusion of gyroscope correction and visual PID control mechanisms. Leveraging a strategically positioned eagle-eye perspective camera, the system gained crucial insights for navigation. To ensure the uninterrupted execution of planned trajectories, the system employs the Message Queuing Telemetry Transport (MQTT) protocol. This technology ensures smooth communication and coordination of actions. The experimental validation of the proposed strategy highlights its efficacy, positioning it as a promising solution for modern warehouse automation needs. By advancing the capabilities of mobile robots within warehouse contexts, this research not only addresses immediate operational demands, but also paves the way for broader applications across various other fields. The developed system enables robust detection and successful path traversal to the designated spot through a position control operating at average of 12.3 rad/s.

INDEX TERMS Control systems, navigation, robot motion, visual control.

I. INTRODUCTION

Mobile robots can improve productivity under several conditions. Industrial and nonindustrial applications, such as planetary exploration, patrolling, and personal services, are possible with the advent of mobile robots. It has the ability to move autonomously, i.e. without the aid of outside human operators in an industrial facility, a lab, on the surface of another planet, etc. A robot that can independently determine, aided by a perception system, the tasks required to accomplish a task is deemed autonomous. In order to coordinate all the robot's components, it also needs a cognitive unit and control system. Siegwart and Nourbakhsh proclaimed that the foundational components of mobile robots are movement, perception, cognition and navigation [1]. Rubio et al. reviewed various aspects of mobile robotics, such as cognition, locomotion, motion planning, navigation, perception and sensing [2].

Hercik et al. convey that a mobile robot's purpose is to function with the production line, take control of the finished goods and then deliver them. The focus of the experiment was on establishing communication between the mobile robot and the manufacturing line, as well as verifying the precision of moving the robot to each position [3]. Geest et al. stated that warehouses aim to cut costs and failures while improving the warehouse's overall productivity, efficiency, and quality of service [4]. The present study examines the necessity of implementing a robotic solution in modern warehouse automation to enhance productivity with a cost-cutting strategy.

This research proposes a novel approach that makes use of a differential drive robot without encoders on its motors

The associate editor coordinating the review of this manuscript and approving it for publication was Yangmin Li.

to satisfy this requirement specifically. The goal of the suggested approach is to achieve point-to-point traversal by combining a visual proportional integral derivative controller with a PID gyroscope correction. The robot can conduct precise lateral and longitudinal corrections during movement with a combination of dual-PID controllers. By minimizing the reliance on expensive encoder setups, the proposed method achieves precise motion control. It integrates a visual PID control system for longitudinal movement regulation and a gyroscope-based control system for lateral control. This fusion results in a dual PID system capable of dynamic trajectory planning, facilitating accurate point-to-point traversal. The system leverages a camera and a cost-effective IMU sensor to reduce encoder dependence. Validated in a simulated warehouse-like environment, this approach demonstrates its potential to revolutionize mobile robot navigation across diverse applications.

The Dual PID and Lateral Motion Management with Gyroscope-based Control System (DPLNS) addresses critical gaps in autonomous path planning for warehouse robots. Conventional methods relying on encoders for precise trajectory planning incur high costs, especially when scaling up robot fleets. The absence of encoders leads to unreliable localization, limiting overall system effectiveness. The DPLNS introduces an innovative gyroscope-based control system for lateral motion, mitigating encoder-related challenges.

The integration of visual PID control and gyroscope-based control results in a dual PID system, enabling dynamic trajectory planning for mobile robots. This approach ensures precise and dependable point-to-point navigation. The system incorporates a cost-effective Inertial Measurement Unit (IMU) sensor and a camera, reducing dependence on encoders while maintaining high performance. This work significantly differs from existing literature by offering a practical solution to encoder-related challenges, enhancing overall autonomy and efficiency in warehouse environments.

The research contributions of the proposed work are as follows:

- Thorough exploration of the cost-effective replacement of encoded motor setups while maintaining precision in motion control, alleviating the necessity for encoders altogether.
- Introduction of the innovative dual PID control system by seamlessly combining visual and gyroscope-based controls, enabling dynamic trajectory planning for precise point-to-point traversal in mobile robots.
- Development and validation of the proposed Dual PID based low-cost navigation system (DPLNS) in a simulated warehouse-like environment, effectively reducing encoder dependency through integration of a camera and an economical IMU sensor.

A. ORGANISATION OF PAPER

The subsequent sections are structured as follows: Section II of the research work begins with an analysis of related publications. Section III focuses on the proposed system's working environment, hardware design, object tracking, and networking components. Section IV describes the experiments, system identification of the gyroscope system, and the final implementation of the DPLNS along with the experimental results. Finally section V concludes the paper with future scope.

II. RELATED WORKS

Several research efforts have been dedicated to automating warehousing processes and improving the efficiency of supply chains. Rahul proposed the concept of swarm intelligence with mobile robots for intelligent warehousing [5]. This work highlights the benefits of mobile robotics for optimized space utilization, reduced retrieval time, decreased power consumption and overall improvement in efficiency.

There are many types of mobile robots in which Myint and Win focused on the position and velocity control of a two-wheel differential drive mobile robot in an obstacle-free indoor environment [6]. This study aims to mitigate position errors during point-to-point motion tasks by utilizing odometry and a PID controller. Leena and Saju proposed a thorough model of a differential drive robot that takes into account the kinematics, actuator dynamics, and rolling resistance of wheels. Smooth trajectory tracking is made possible through controller design. The model and control method has been found to provide accurate trajectory tracking for a variety of different trajectory types that mimic real-life conditions [7].

The PID controller is an efficient controller for controlling and stabilizing the state variables of a system. Al-Shabi proposed a system of using a closed-loop PID controller with feedback from motor encoders for a 2 DOF robotic arm that solved overlapping input problems in both joints of the robotic arm [8]. Capito et al. implemented, tested and evaluated the performance of different control algorithms for monitoring trajectories for mobile robots. The control techniques employed include a PID controller and a sliding mode controller. Each control scheme is built, taking into mind the robot's model.

The PID and the sliding mode controller employ a reduced-order model, which is obtained considering the mobile robot platform as a black box. All the controllers are evaluated and compared, initially by simulations and subsequently by utilizing a Pioneer 3-DX robot in field experiments. Systematic errors in point-to-point motion tasks arise when there are consistent and predictable deviations in the robot's orientation and position [9]. A controller based on output feedback linearization was presented by Montoya-Villegas et al. Its output function is a linear combination of the error states. The controller's local asymptotic stability is confirmed in the study, and the Pioneer 3-DX robot is used to evaluate the methodology [10]. To control this error, the PID is applied over the gyroscope and visual feedback.

In the virtual robot experimentation platform environment, Morales et al. presented the application of several intelligent controllers based on Learning Algorithm for Multivariate

Data Analysis (LAMDA) to carry out the task of tracking the trajectory of a mobile robot Pioneer 3-DX. The research recommends the creation of a cascade control method made up of two controllers: an internal controller applied to the robot dynamics using LAMDA techniques, and an external controller based on feedback linearization for the robot kinematics [11].

Borenstein et al. and Sakpere et al. used a variety of methods and sensors, including the inertial navigation system, Global Positioning System (GPS), global navigation satellite system, monocular and stereo cameras, active beacons, RFID-based devices, and odometers, to obtain robot posture information [12], [13]. Dobrzanska and Dobrzanski proposed an automatic correction system that can be implemented using measurements from a laser rangefinder. The laser rangefinder continuously scans the surrounding environment and provides real-time distance measurements to nearby objects. By comparing these measurements with the Automatic Ground Vehicles (AGV) expected position based on its planned trajectory, any deviations can be identified [14]. Currently, one of the most efficient and trustworthy techniques used for relative localization is Visual Odometry (VO).

Zhang et al. used a Pioneer 3-DX platform in order to evaluate an adaptive visual servoing approach for controlling the mobile robot to the required position. The system error vector is chosen as the quantifiable values that can be recovered using a motion estimation approach, taking into account the model uncertainty [15]. Pati and Kala developed and tuned a PID controller for a mobile robot, emphasizing its significance in achieving accurate and robust robot control with vision [16]. Rubio et al. provided a comprehensive overview of mobile robots, exploring various techniques of planning and mapping their paths using perception [2]. Aqel et al. and D'Orazio et al. analyzed the appearance changes that motion causes in the images taken by the passive cameras attached to it, VO makes it possible to incrementally estimate the pose of the robot [17], [18].

Furthermore, Hmeyda and Bouani. presented an intelligent approach for detecting static obstacles and generating an optimal and safe path for an autonomous mobile robot using image processing and a PID controller [19]. This study leverages a USB camera to capture the robot's environment, extract positions of the robot, goals, and obstacles, and generate an optimized path. Farkh and Aljaloud presented a line-tracking robot with a camera, image processing software, and a PID controller. The line is detected by the camera, features are extracted from the image using image processing software, and steering and speed commands are calculated using a PID controller [20]. Malik et al. has presented an PID based approach for the development of a camera-based positioning system for quadrocopters, focusing on automating the landing process. This work outlines the process of identifying relevant plant dynamics using black-box system identification [21]. Chinthaka et al. introduced a novel method for self-position estimation and hovering control of a small aerial robot using a downward-facing camera and a microcontroller, utilizing the tile corners on the indoor floor as existing features to estimate the robot's position and orientation. Authors also devise a lightweight image processing algorithm that can run on the microcontroller in real time. The performance of this method is evaluated on an actual drone and demonstrate its accuracy and efficiency [22].

Cumani and Guiducci proposed a fast Hessian-based feature descriptor to refine the image localization of features in VO images. Then the motion is estimated using a robust bundle adjustment of matched feature points that are independently derived from two pairs of stereo images [23], [24]. For VO computation, Nourani-Vatani et al. used a single downward-facing camera fixed to a ground vehicle. The process of motion estimation can be deconstructed into a distinct forward/backward translation component and a distinct rotation component centered around the rear wheel axle. This delineation underscores the rationale behind the authors' utilization of optical flow information and an Ackerman-like steering model, aimed at optimizing the efficiency of this process [25].

Patruno et al. determined the relative posture of an AGV that moves in a structured environment using an embedded vision system based on laser profilometry. The authors connected the laser signatures that were retrieved by processing successive photos to estimate the relative robot displacements along the direction of movement [26], [27], [28]. Adrian and Constantin proposed a design for an omnidirectional robot that makes Pulse Width Modulation (PWM) adjustments in four motors in response to the orientation recorded from the gyroscope using a PID controller [29]. Xiong et al. and Zhou et al. discussed issues of using a Kalman filter, which includes divergence issues of measurement functions and is suitable for mobile localization with Gaussian noise models [30], [31].

Havangi proposed an unscented Kalman filter for resolving issues with the Kalman filter and for the localization of mobile nodes in non-line-of-sight scenarios [20]. Aguiree-Castro et al. designed a remotely operated vehicle specifically tailored for underwater exploration purposes using a gyroscope sensor along with a PID controller for error correction [31]. To establish uninterrupted communication between masters and slaves, Mishra and Kertesz proposed the utilization of MQTT. This messaging transport protocol holds authorization from OASIS and ISO (ISO/IEC PRF 20922). According to the results of this survey, MQTT stands out as one of the Internet Of Things (IoT) protocols that is most widely used [30].

Diddeniya et al. described a service robot navigation system involving the MQTT protocol. It enables real-time updates of robot states for multiple users and serves as the foundation for this system [32]. The robot can effectively navigate to predetermined locations and identify target people with high accuracy due to the adoption of this technology.

The performance of the MQTT and CoAP communication protocols in the context of catastrophic multi-robot situations is compared in the research work by Yamin et al. [34]. The results show that, when compared to CoAP in the Within the Ultra Narrowband Radio Pulse Function (UNR-PF) data transmission environment, the MQTT Protocol demonstrates a pronounced advantage in real-time communication, attributable to its elevated data transfer rate. Furthermore, MQTT boasts a user-friendly nature and seamless integration capabilities within the UNR-PF framework. It is noteworthy to highlight that MQTT operates on the TCP/IP protocol, in contrast to CoAP which employs UDP, thus rendering CoAP superfluous for error correction purposes.

The proposed DPLNS work aims to address few research gaps related to autonomous path planning for robots operating in warehouse environments. One significant gap was observed in the conventional method used to achieve precise point-to-point trajectory planning in mobile warehouse robots. The conventional approach typically involves the use of encoders on motors to provide feedback control. However, implementing encoders in the system incurs substantial costs, particularly when scaling up the fleet of mobile robots to a larger size. The absence of encoders poses a challenge in obtaining accurate information about actual motor speeds. In the absence of encoder feedback, the information is confined solely to the commanded speed, thereby introducing a considerable degree of unreliability in the task of localization. This limitation hampers the overall effectiveness and efficiency of an autonomous path planning system. An innovative control system based on gyroscope has been implemented to effectively manage lateral motion. This approach harnesses the yaw data from the gyroscope to achieve accurate control over sideways movement.

The fusion of the visual Proportional-Integral-Derivative (PID) control system and the gyroscope-based counterpart has led to the development of a dual PID system. This combined system empowers dynamic trajectory planning for mobile robots, thereby guaranteeing precise and dependable point-to-point navigation capabilities. The proposed DPLNS was introduced by incorporating a camera and a cost-effective Inertial Measurement Unit (IMU) sensor. This strategic integration reduces the system's dependence on encoders while maintaining a high level of performance.

III. PROPOSED SYSTEM

The proposed system utilizes a dual PID control approach that switches between the gyroscope and the visual feedback system. The robot works in indoor conditions, and for testing, a banner with a grid of black squares is used, as shown in Fig. 2. The main goal of this work is to provide robots with accurate motion control. Gyroscope-based PID adjustments are used to achieve sharp turns greater than 45°, providing precise and stable rotational movements. In contrast, the visual PID system is used to maintain a straight line and successfully reach a given destination, as visualized in Fig. 3. This enables the robot to steer as needed, based on visual feedback, ensuring that its trajectory follows the intended course. The whole proposed system is illustrated in Fig. 1 and Fig. 2.

As depicted in Fig. 2, the implemented robotic system boasts a sophisticated autonomous navigation control scheme. The process initiates with the system utilizing visual input to meticulously define boundaries and generate an optimal path from the predefined start to end points. Subsequently, the robot adeptly tracks this path, relying on continuous visual feedback to modulate motor PWM signals, facilitating a seamless and fluid motion.

Noteworthy is the system's adaptive response to 90-degree turns, showcased in Fig. 3. During such turns, a smooth transition to gyroscope-based control takes place, ensuring a level of precision and stability that is notably superior. This gyroscope-based control mechanism is crucial for navigating sharp turns, contributing to the system's overall efficiency and effectiveness in challenging spatial scenarios. Upon successful negotiation of the turn, the system seamlessly reverts to visual control, opting for a less abrupt trajectory to efficiently approach the predetermined drop-off point. The careful adjustment of PWM signals at this stage is pivotal, facilitating the robot's ability to come to a precise halt when executing the package release operation. This level of precision in both navigation and payload handling underscores the robustness and versatility of the implemented robotic system, making it well-suited for applications in complex and dynamic environments

A. OPERATING ENVIRONMENT

The navigation system of the robot operates on a white floor with a black square grid layout, as presented in Fig. 4. A colored sheet is attached to the robot's top panel to rack its position using a visual feedback system. The camera is positioned three meters above the ground to provide an eagle-eye perspective hat captures the grid environment of the robot. The camera can transmit video at a resolution of 1080p quality and a frame rate of 30 frames per second. A USB 3.0 cable was used to connect the camera to the host laptop, enabling quick data transfer.

B. HARDWARE DESIGN

The robotic system developed for this study includes a differential mechanism made up of two motorized wheels along with two driven wheels, which are then connected to a dummy shaft to enable unrestricted movement. A 3 mm aluminum sheet was used to build the chassis of the robot. Four spacer screws were used to link the top panel and the chassis. The top panel contains the package-dropping mechanism, and the color sheet covers 70% of the area of the top panel. The bottom panel houses the L298n motor driver, four 18650 batteries, the MPU6050 inertial measurement unit, and the Nodemcu controller. Four individual L clamps were mounted on the bottom of the chassis to firmly fasten two 300 RPM geared motors and two dummy shafts, respectively.

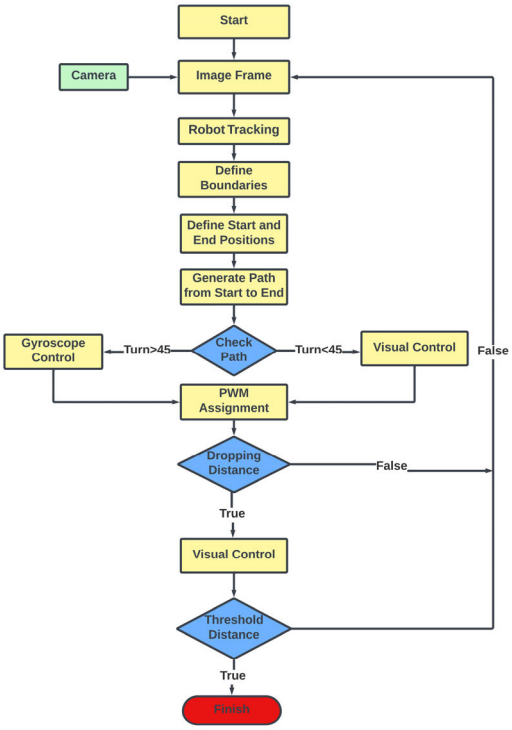

FIGURE 1. Workflow of the proposed work.

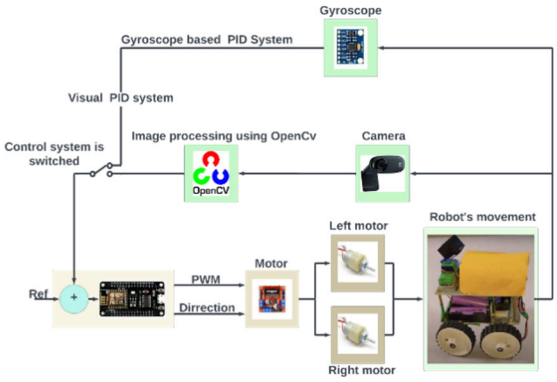

FIGURE 2. Block diagram of the Proposed Work.

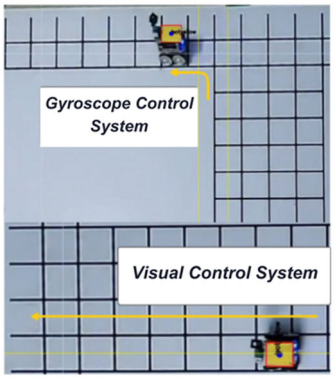

FIGURE 3. Illustration of dual control mechanism.

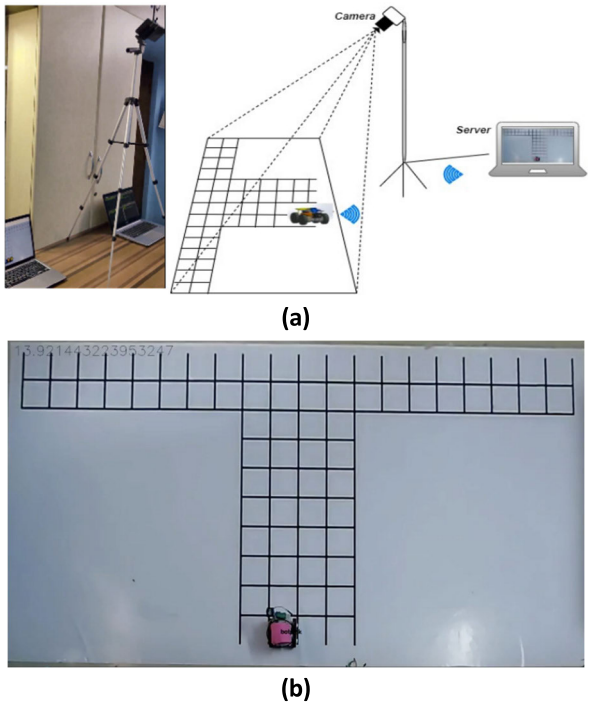

FIGURE 4. Environmental setup of the proposed work.

Individual L clamps are used to firmly fasten each motor to the chassis base plate.

A servo and a 3D-printed mount were used to design a mechanism for carrying the sample package, which was released at the predetermined target area. Fig. 5(b) demonstrates the different hardware components used for the construction of the robot. Fig. 5(c) and Fig. 5(a) represent the fully constructed robot's CAD model and the real image.

C. PREPROCESSING

In this research, we used the warping technique to preprocess the input video frames. Warping is a basic image processing method used to change a picture taken from a slanted angle (as seen by the camera) into a straight-down view, such as looking from above. The main goal is to fix any weird distortions caused by the original angle and obtain a clear, accurate representation of the scene. This kind of view is helpful for things like helping robots move around, finding objects and planning their paths. The before and after the perspective transform is illustrated in Fig. 6.

Given the coordinates of the following points in the captured image:

- Four corners of the green rectangle on the track, denoted by points (50,0), (150,0), (0,200), and (200,200).
- Corresponding points in the desired warped image, denoted by points (0,0), (200,0), (0,200), and (200,200).
- The homography matrix (H) can be computed based on these corresponding points. Subsequently, a homography matrix was employed to perform the perspective

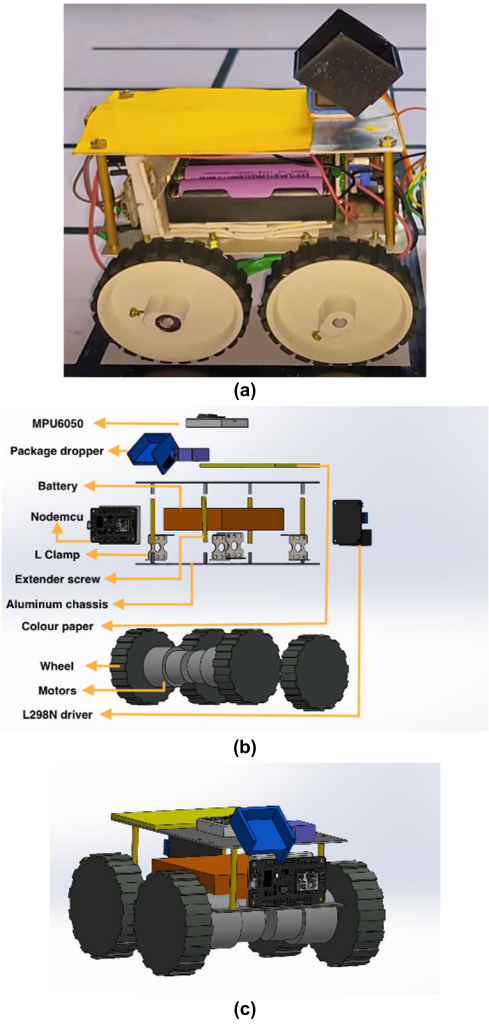

FIGURE 5. (a). Real Robot (b). Labelled View of Robot (c). CAD Model of Robot.

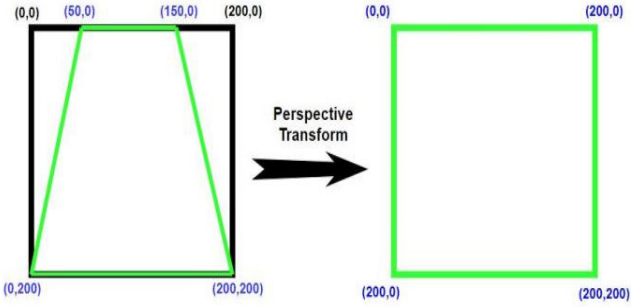

FIGURE 6. Perspective transform of the eagle eye view.

transformation on each frame of the video, yielding the warped image.

The transformation equation is presented in Eq. 1.

$$\begin{bmatrix} X^{|} \\ Y^{|} \\ 1 \end{bmatrix} = \begin{bmatrix} h_{11} & h_{12} & h_{13} \\ h_{21} & h_{22} & h_{23} \\ h_{31} & h_{32} & h_{33} \end{bmatrix} \begin{bmatrix} X \\ Y \\ 1 \end{bmatrix} \quad (1)$$

where:

- (X, Y) are the coordinates of a point in the original image.
- (X', Y') are the coordinates of the corresponding point in the warped image.

The homography matrix H is a 3 × 3 matrix with the elements determined based on the corresponding points in the original image and the desired warped image. It can help improve the accuracy and efficiency of the robot's navigation system by correcting for perspective distortion and making it easier to identify objects and plan paths.

D. OBJECT TRACKING AND VISUAL CONTROL SYSTEM

The system begins by capturing video frames from a camera source and applying perspective transformation to obtain a top-down view of the lane. This transformation allows for more accurate lane detection. Following the transformation, the frames undergo image processing using OpenCV, including Gaussian blur and conversion to HSV color space. This enhances the detection process by reducing noise and improving color detection. The system then detects colored objects representing the lanes using color thresholding techniques and calculates their center positions based on the contours and bounding rectangles. To facilitate lane correction, a PID controller is initialized with predetermined parameters, such as proportional, integral, and derivative gains (K_p, K_i, K_d) as well as the desired setpoint and sample time. Intially transfer function for the system is obtained by plotting pwm difference between left and right motor and distance of robot's center with defined path and finding nearest fit transfer function of that plot. Once transfer function is defined the system was tried with P, PD controllers.But with P controller the robot was wobbled about the defined line and in case of PD controller the robot had overshoot error. The PID control algorithm is applied using the current lane center position and the desired setpoint to calculate the appropriate steering input.

This computed steering input is then used to control the vehicle's motors. The system generates individual PWM signals for the left and right wheels based on the calculated steering input. These PWM signals determine the power or speed of rotation for each wheel, enabling the vehicle to make precise steering adjustments and maintain its position within the lane. The system utilizes motor control signals published through an MQTT client to control the vehicle's motors and keep it within the desired lane. Actions such as 90, 180 degree turns are determined based on the lane positions, and corresponding commands are sent to the vehicle's control system by operating in a continuous control loop. The system captures frames, detects lane positions, applies PID control and sends motor control signals, ensuring the vehicle maintains its position within the desired lane.

E. GYROSCOPE INTEGRATION

The main system implemented in this research switches to the gyroscope system when the robot needs sharp turns.

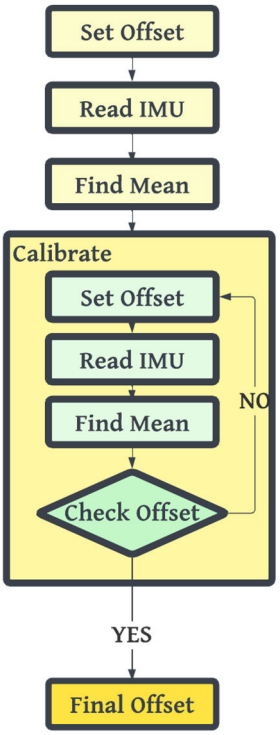

FIGURE 7. Offset calculation.

1) READING YAW VALUES

To determine the orientation of the robot, MPU6050 was used. It is an IMU that integrates a MEMS (Micro Electro Mechanical Systems) gyroscope and an accelerometer that transmits data over a conventional I2C interface [1]. Due to the inherent misalignment between the IMU installed on the robotic platform and the reference plane of the ground, it is necessary to perform calibration procedures on the data obtained from the MPU6050 sensor. As a result, a series of data measurements from the accelerometer and gyroscope were made to produce offsets. As presented in Fig. 7, these offsets are determined by an iterative process. A translation from the body frame to the inertial frame is offered via offsets.

The inertial frame serves as the reference coordinate system for all calculations involving angles and velocities, whereas the body frame pertains to the orientation and movement of the robotic entity itself. All accelerometer and gyro offsets were set to zero at the start of the procedure. The mean value of each offset is then computed using thousand IMU readings. The new offsets are then created by entering these values into the IMU. Until the offsets are within a predetermined tolerance, the calibration process will keep taking the mean IMU values. The correct values for the accelerometer and gyroscope were then obtained by manually entering these offsets.

The Digital Motion Processor (DMP) of the MPU6050 is utilized to offload processing from the CPU. An internal buffer combines information from the IMU to determine the orientation. The DMP performs sensor fusion algorithms internally and stores the relative orientation in its buffer. Fig 8 illustrates the internal buffer format of the DMP. Initially, orientation is calculated in Quaternions and then converted to Euler angles using Eq. 2.

$$\begin{bmatrix} \Phi \\ \theta \\ \psi \end{bmatrix} = \begin{bmatrix} arctan\left(\dfrac{2(q_w q_x + q_y q_z)}{1 - 2(q_x^2 + q_y^2)}\right) \\ \sqrt{\dfrac{1 + 2(q_w q_y - q_x q_z)}{1 - 2(q_w q_y - q_x q_z)}} \\ arctan\left(\dfrac{2(q_w q_y + q_x q_y)}{1 - 2(q_y^2 + q_z^2)}\right) \end{bmatrix} \tag{2}$$

Where:

Φ - *Roll* $\quad Q = [q_x, q_y, q_z, q_w] = \vec{q}_v + q_w$

Θ - *Pitch* $\quad Q$ *is Quaternion Representation of an angle*

Ψ - *Yaw* $\quad \vec{q}_v = q_x\hat{i} + q_y\hat{j} + q_z\hat{k}$

$\vec{q}_v$ - *Imaginary Part*

q_w – *Real Part*

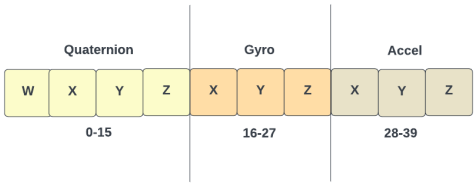

FIGURE 8. Data organization of the DMP buffer.

2) PID CONTROL SYSTEM

Intially transfer function for the system is obtained by plotting pwm difference between left and right motor and angle of robot and finding nearest fit transfer function of that plot. The error computed from the system is multiplied to a K_p,constant in the proportional controller, which scales the error and directly affects the PWM output. A bigger inaccuracy causes the motors' PWM output to increase, which speeds up orientation correction. The differential controller is implemented to reduce the system's sensitivity to changes in error and to dampen the system output by taking the error's rate of change into account. The differential controller responds to the rate of change in the orientation error to help stabilize the system. An integral controller is implemented to eliminate small errors that the P term alone might not be able to address, which accounts for any steady-state error and accumulates over time. An integral controller is implemented to eliminate small errors that the P term alone might not be able to address, which accounts for any steady-state error and accumulates over time. Fig. 9 represents the detailed flow of the implemented PID system.

The system implemented in this research is constrained by factors such as motor voltage, speed restrictions and the PWM duty cycle. Because of these restrictions, the control system becomes saturated, which prevents the output from going beyond predetermined limits. The main issue here is integrator windup. The integrator keeps integrating the error

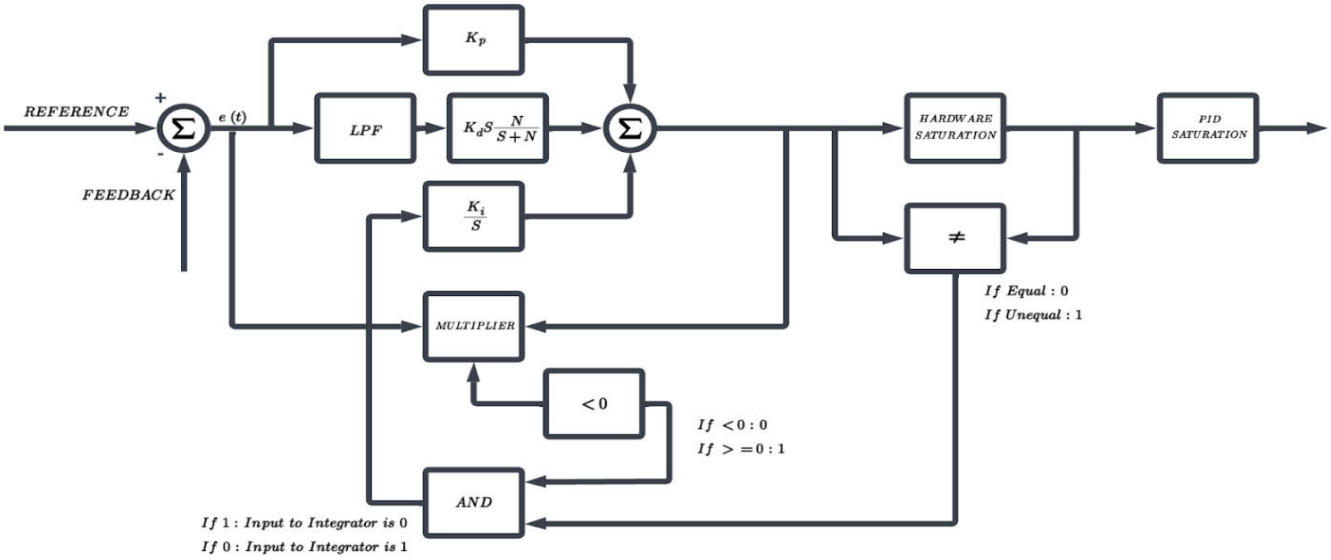

FIGURE 9. PID implementation.

as the commanded input approaches the saturation limit, which causes overshoot and instability. Anti-windup loops are attached to the integral controller to overcome this issue. An additional condition is added to prevent clamping when the PID controller is trying to decrease the output and come out of saturation. The result is a stable response with no overshoot, and the integrator performs well even when the reference is set to zero. If the motor's top speed is unknown, demanding a PWM difference that is too high will cause the integrator to wind up, delaying the reaction when the speed is reduced. By stopping the integrator when the commanded PWM difference exceeds the motor's maximum acceptable.

PWM difference, the clamping approach can address this issue. Instability can result from the differentiator term's tendency to magnify high-frequency noise. To fix this, a 95 KHz low-pass FIR filter was added to the differentiator term to reduce the high-frequency components.

F. NETWORKING

The networking configuration of the bot is based on the MQTT protocol, which enables communication between the bot and the server. The bot is equipped with an ESP8266-based module, which establishes a Wi-Fi connection to the server's network. Once connected, the bot establishes a connection to the MQTT broker specified by the IP address of the server. This connection allows the bot to publish and subscribe to topics, enabling bidirectional communication. The bot is configured to subscribe to a specific MQTT topic unique to each bot, where it receives commands and instructions from the server. The message payload received is processed by the callback function, which performs actions based on the received commands. The bot receives PWM values for both the left and right motors from the visual PID system and other supplementary commands for servo actuation. Additionally, the bot publishes status updates and information to the server, providing real-time feedback and monitoring capabilities.

IV. RESULTS AND DISCUSSION

A specially created robot outfitted with an MPU6050 IMU unit, L298N motor driver, two encoderless geared motors, four 18650 batteries, and a NodeMCU module was used to assess the proposed DPLNS. The experiment is initiated by providing a sample PWM input. The resulting output is closely monitored to characterize the underlying system dynamics. Through this analysis, the system's mathematical equation is identified. Subsequently, a PID controller is tuned to optimize the system's performance, aiming to minimize overshoot and achieve rapid settling time.

A. EXPERIMENT INTIALIZATION

In order to perform an experimental investigation, the model equation of the gyroscope system and visual system is derived in response to the PWM difference between the left and right motors. In the study of the gyroscope system, a square-shaped PWM input was employed with a constant amplitude of 50 units, alternating between high and low states within a 8300 millisecond time period, as shown in Fig. 10 (a). This well-defined input profile was utilized to investigate the change in orientation of the robot with respect to PWM difference input, as shown in Fig. 11(a). During the experimental analysis, it was observed that the robot's orientation changes from + 180 to −180 degrees. The robot achieved this full range of orientation by taking 3200 seconds to rotate from 0 to −180 degrees and 6400 seconds to complete the rotation from 0 to + 180 degrees. Similarly, in the study of the visual system, a step-shaped PWM difference input was employed with a constant amplitude of 50 units for

12.6 seconds, as shown in Fig. 10 (b). This input profile was utilized to investigate the change in distance of the robot from reference with respect to PWM input, as shown in Fig. 11 (b). In the absence of any PWM difference applied to the motors, the robot exhibited a motion away from the reference line in the negative direction. However, when a PWM difference was introduced to the motors, the robot started to deviate in the positive direction relative to the reference line.

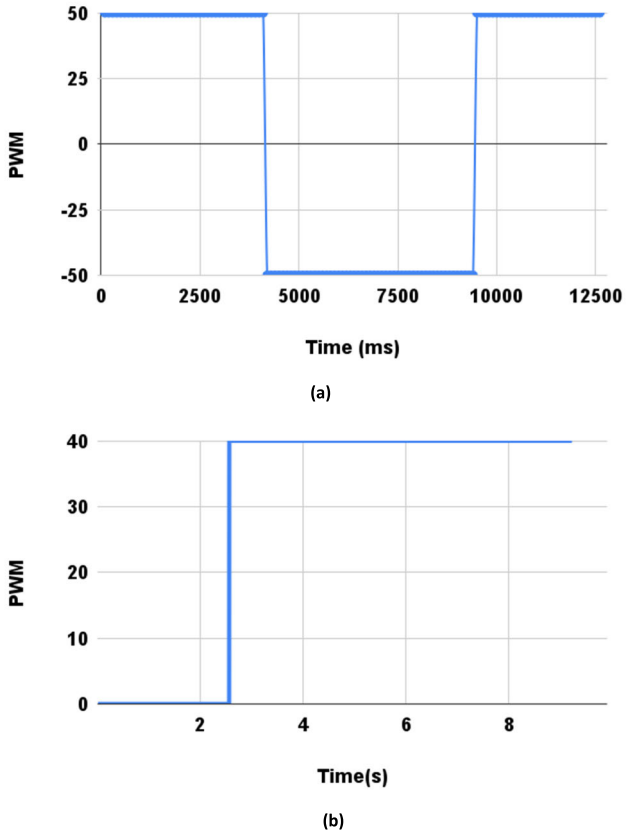

FIGURE 10. PWM input for (a) Gyroscope system (b) Visual system.

B. SYSTEM IDENTIFICATION OF GYROSCOPE SYSTEM

A nonlinear least squares approach was employed, coupled with an automatically chosen line search algorithm, to ascertain the optimal fit transfer function (Eq. 3) corresponding to the input and output data represented in Fig. 12. The system is accurately represented by Eq. 3, with the best-fit obtained showing a 89.24% agreement with the experimental data, as demonstrated in Fig. 12. Throughout the iterative process, the algorithm was allowed to run for 20 iterations, converging to the best-fit transfer function with minimal prediction error and mean square error. The final prediction error of the best-fit model was determined to be 118.8, while the mean square error stood at 107.7. The derived transfer function reveals insightful information about the system's behavior. Specifically, the identified pole of the best-fit model is found to be -1.062, indicating a damping factor and an

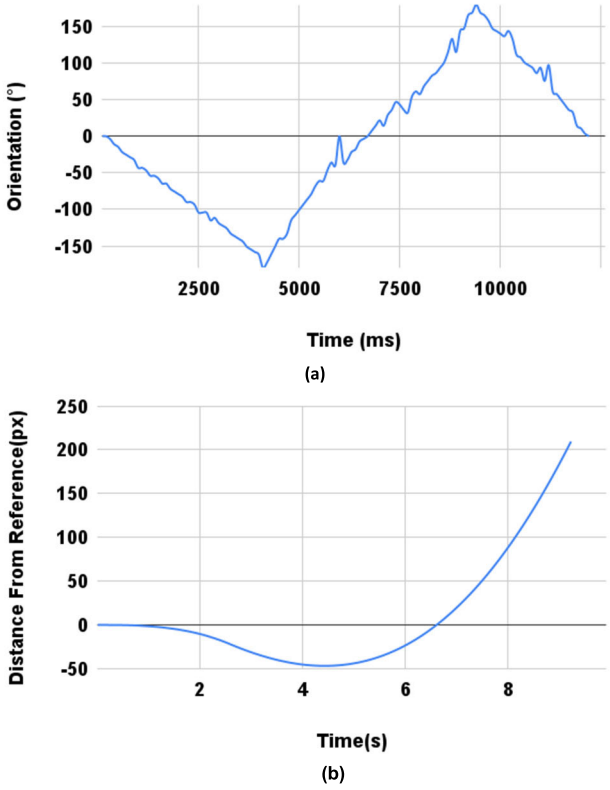

FIGURE 11. (a) Tracked orientation (b) Distance from reference.

inherent dynamic response. Additionally, the system exhibits two complex-conjugate zeros located at $-0.0732 + 0.1168$i and -0.0732 - 0.1168i, suggesting an oscillatory response.

To further validate the characteristics of the system, the poles and zeros diagram Fig. 13 was constructed, providing a graphical representation of the transfer function's complex plane. The observed step response of the system Fig. 14 is also depicted, illustrating the system's dynamic behavior in the time domain.

$$G(S) = \frac{-10.48S - 11.13}{S^2 + 1.464S + 1.903} \tag{3}$$

C. PID TUNING OF GYROSCOPE SYSTEM

The control system's performance was systematically optimized by incorporating an auto tuned PID controller, leveraging MATLAB's PID Tuner App, to achieve the desired system behavior. The tuning process yielded controller parameters K_p, K_i, K_d shown in Table 1 effectively met the performance objectives, enabling the system to exhibit rapid response characteristics with minimal overshoot and settling time. Upon implementing the autotuned PID controller, the overall system demonstrated a highly satisfactory step response, as depicted in Fig. 15. This result reinforces the efficacy of the selected PID controller parameters in effectively regulating the system's behavior. Furthermore, the performance analysis revealed impressive gains and phase margins for the system.

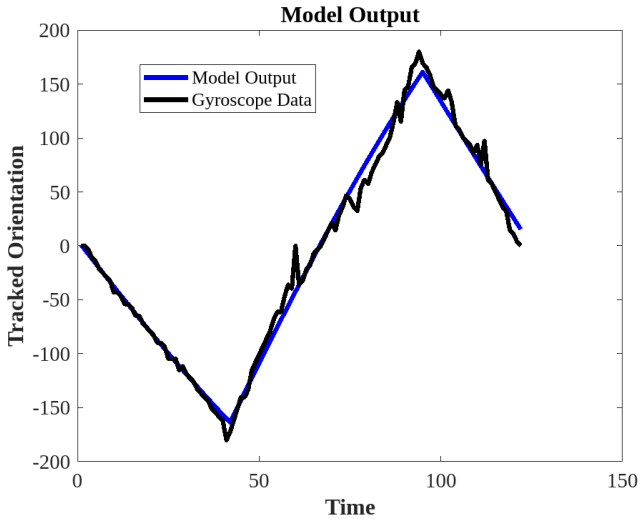

FIGURE 12. Model output of the gyroscope system.

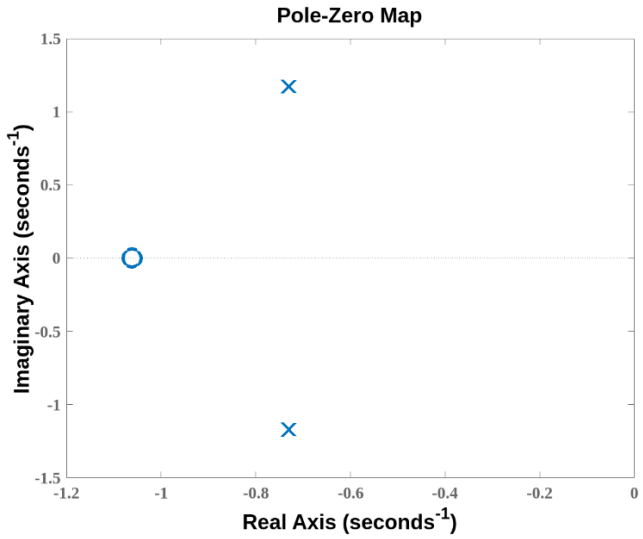

FIGURE 13. Pole and zeros of the gyroscope system.

TABLE 1. Tuning parameters for the gyroscope system.

Parameters	Values
K_p	-1.295
K_i	-5.057
K_d	0.0798

Specifically, the system achieved a gain margin of 7.2 dB at a frequency of 12 rad/s, indicating robust stability and control. Additionally, a significant phase margin of 75.8 degrees was attained at 14.2 rad/s, further affirming the system's stability and ability to handle external disturbances effectively.

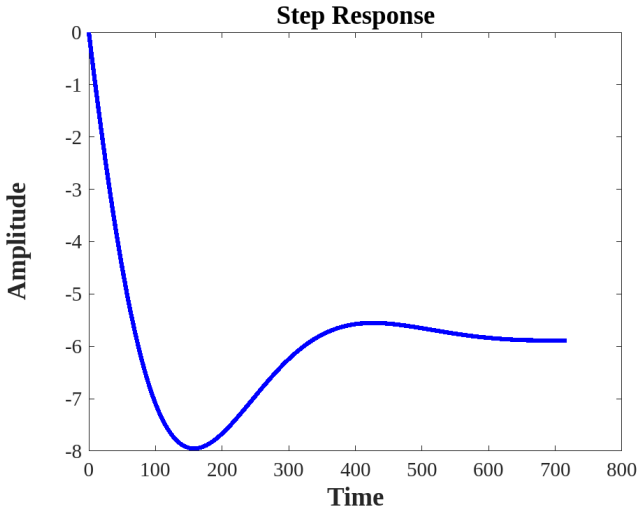

FIGURE 14. Step response of the gyroscope system before tuning.

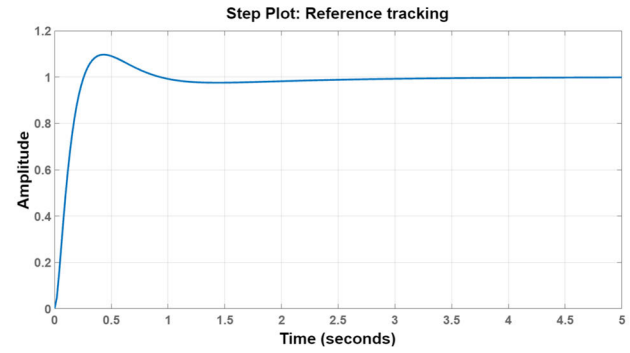

FIGURE 15. Step plot of the tuned gyroscope system.

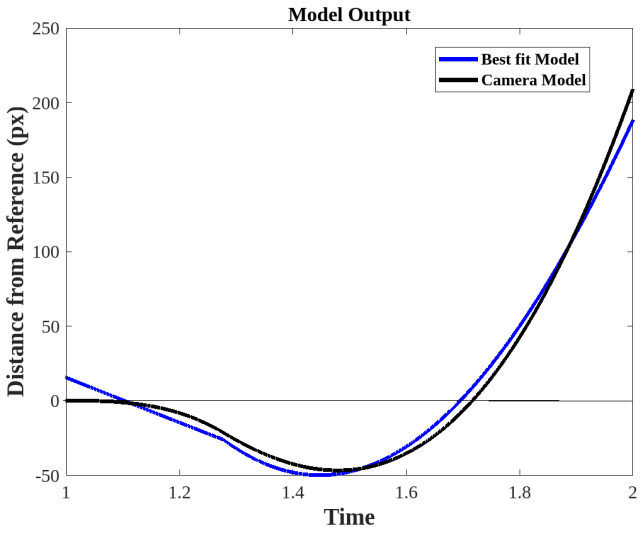

FIGURE 16. Model output of visual system.

D. SYSTEM IDENTIFICATION OF VISUAL SYSTEM

The sequential quadratic programming algorithm was successfully implemented to determine the best-fit transfer

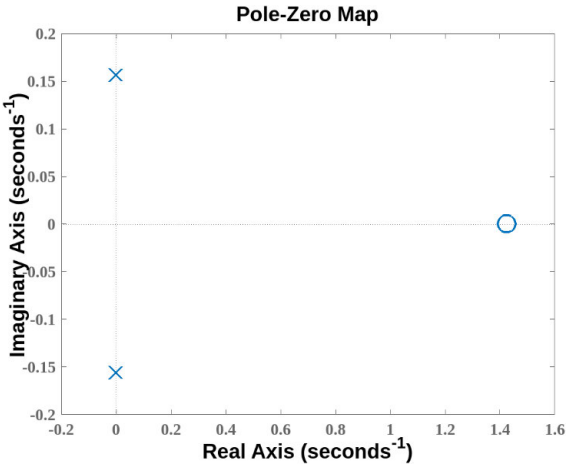

FIGURE 17. Poles and zeros of the visual system.

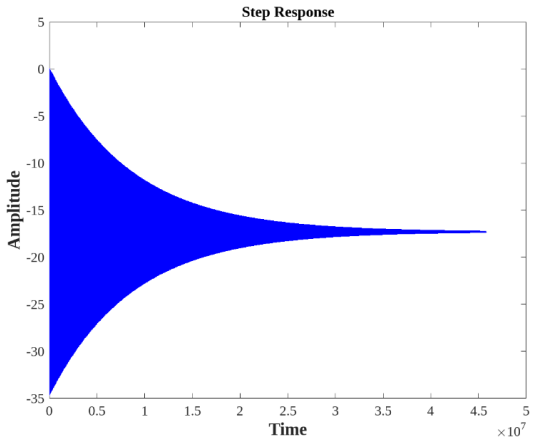

FIGURE 18. Step response of visual system before tuning.

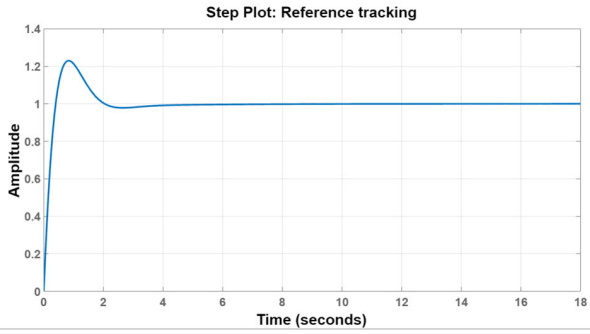

FIGURE 19. Step plot of the tuned visual system.

function, as denoted in Eq. 4. The algorithm was iterated for 40 cycles, and the best-fit transfer function achieved an accuracy of 87.71%, as graphically presented in Fig. 16. The final prediction error of this best-fit model was found to be 58.41, with a mean square error of 58.21, indicating an accurate representation of the system's dynamics. Upon analyzing the identified transfer function, it was found that the system exhibits a pole at 1.4288, indicating a dominant time constant that significantly influences its transient response. Furthermore, the system possesses a pair of complex conjugate zeros at ±0.1562i, suggesting a characteristic oscillatory behavior. This information is graphically illustrated in Fig. 19 through a pole and zeros diagram. The step response of the overall system after including the PID controller is illustrated in Fig. 20.

$$G(S) = \frac{0.2715S - 0.3863}{S^2 + \left(2.86 * 10^{-7}\right) S + 0.02435} \tag{4}$$

E. PID TUNING OF VISUAL SYSTEM

The control system's performance was systematically optimized by incorporating an auto tuned PID controller, leveraging MATLAB's PID Tuner App, to achieve the desired system behavior. The inclusion of the PID controller significantly improved the system's step response, as demonstrated in Fig. 21. The tuned PID controller with the parameters mentioned in Table 2 demonstrated quick reaction and effective control, ensuring stable and accurate system behavior. The system achieved a gain margin of 5.99 dB at 12.6 rad/s, indicating a margin of stability with respect to the gain variations. Furthermore, a phase margin of 22.5° at 6.24 rad/s was obtained, indicating sufficient stability margins to avoid instability and ensure a well-damped response.

TABLE 2. Tuning parameters for the visual system.

Parameters	Values
K_p	-8.835
K_i	-9.415
K_d	-2.006

F. FINAL IMPLEMENTATION

The implemented robotic system utilizes a sophisticated control scheme to autonomously navigate a predefined path. At the outset, the robot commences its journey from the designated start position and steadily tracks the path by leveraging the visual system's output, which modulates the motor's PWM signal to effectuate smooth movement. Upon encountering a sharp 90-degree turn, precisely depicted in frame 3, the robot seamlessly transitions to a gyroscope-based control. During this phase, the robot acquires PWM data from the gyroscope, enabling it to execute the turn with superior precision and stability. After successfully negotiating the turn, the robot seamlessly reverts to visual control and follows a less abrasive path to efficiently reach its proximity to the targeted drop-off location. To ensure precise placement at the designated drop-off point, the PWM signals were carefully adjusted, allowing the robot to come to a precise halt when releasing the package.

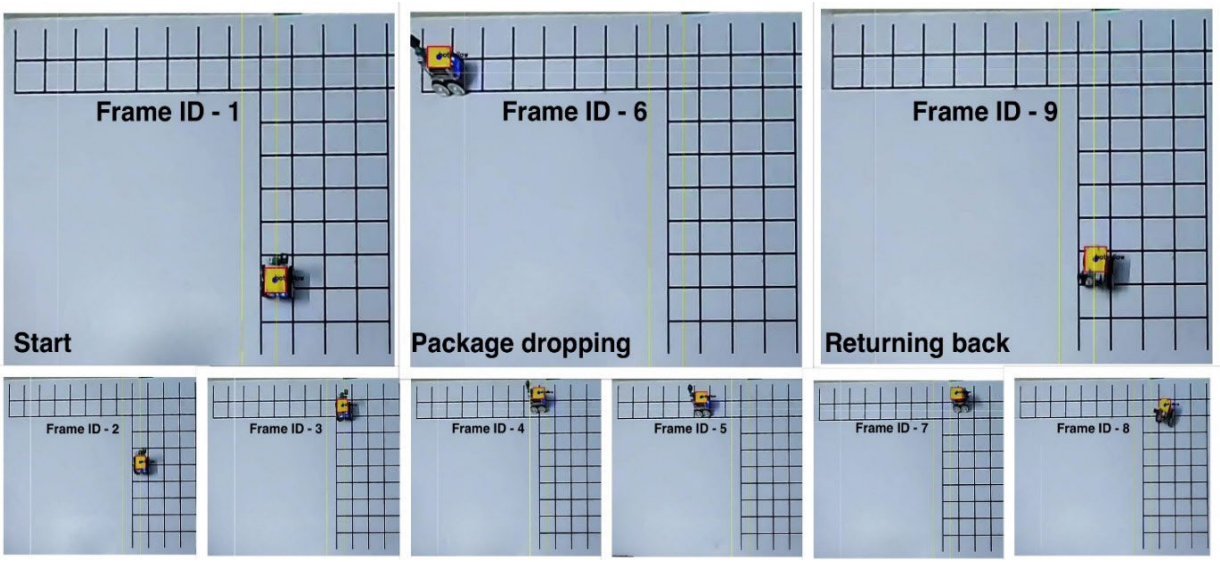

FIGURE 20. Robot movement.

Upon completion of the package drop-off, the robot undertakes a 180-degree turn, which is effectively facilitated by the gyroscope control. This maneuver enables the robot to realign with its initial orientation. Subsequently, the robot intelligently switches between the visual and gyroscope systems, effectively alternating control mechanisms as required to trace its path in reverse. In doing so, the robot successfully navigates back to its original starting position. The seamless integration of visual and gyroscope-based control, coupled with the precise modulation of PWM signals, empowers the robot to exhibit exceptional performance and achieve its intended object.

V. CONCLUSION

This study proposes a novel DPLNS for robot navigation in a warehouse environment. The proposed system achieves precise and economical navigation in the defined environment by using dual PID control and inexpensive sensors. The suggested method enables the robot to achieve accurate and efficient point-to-point traversal, increasing productivity and cost effectiveness in warehouse operations. This was accomplished by merging the visual PID control with the gyroscope correction. The experimental evaluation's findings demonstrate how successfully the system is tuned to navigate the warehouse environment. The addition of an eagle-eye perspective camera and trajectory planning through MQTT improves the robot's capabilities and makes it possible for the planned trajectories to be executed without any problems. The main novelty of this study is the proposed Dual PID control scheme, which effectively combines the advantages of visual and gyroscope-based control. This allows the robot to achieve high accuracy and stability, even in challenging environments. Additionally, the use of inexpensive sensors makes the proposed system more economical than traditional approaches. The experimental results show that the proposed system is able to navigate accurately and efficiently in a warehouse environment. The robot was able to successfully complete a variety of tasks, including navigating through narrow passages, making sharp turns, and dropping off packages at designated locations. One limitation of the proposed system is that it is not yet able to handle unexpected obstacles. In the future, it would be beneficial to develop a more robust obstacle avoidance system. Additionally, the system could be improved by adding more sensors, such as a laser range finder, to provide better environmental awareness. In the future, the system could be further improved by adding more sensors and developing a more robust obstacle avoidance system.

REFERENCES

[1] R. Siegwart and I. R. Nourbakhsh, *Introduction to Autonomous Mobile Robots*. London, U.K.: A Bradford Book, 2004.
[2] F. Rubio, F. Valero, and C. Llopis-Albert, "A review of mobile robots: Concepts, methods, theoretical framework, and applications," *Int. J. Adv. Robotic Syst.*, vol. 16, no. 2, Mar. 2019, Art. no. 172988141983959, doi: 10.1177/1729881419839596.
[3] R. Hercik, R. Byrtus, R. Jaros, and J. Koziorek, "Implementation of autonomous mobile robot in SmartFactory," *Appl. Sci.*, vol. 12, no. 17, p. 8912, Sep. 2022, doi: 10.3390/app12178912.
[4] M. van Geest, B. Tekinerdogan, and C. Catal, "Smart warehouses: Rationale, challenges and solution directions," *Appl. Sci.*, vol. 12, no. 1, p. 219, Dec. 2021, doi: 10.3390/app12010219.
[5] K. Rahul, "Swarm robotics for intelligent warehousing: An application," *Int. J. Res. Eng. Technol.*, vol. 2, no. 10, pp. 518–521, Oct. 25, 2013, doi: 10.15623/ijret.2013.0210080.
[6] C. Myint and N. N. Win, "Position and velocity control for two-wheel differential drive mobile robot," *Int. J. Sci., Eng. Technol. Res.*, vol. 5, no. 9, pp. 2849–2855, Sep. 2016.
[7] N. Leena and K. K. Saju, "Modelling and trajectory tracking of wheeled mobile robots," *Proc. Technol.*, vol. 24, pp. 538–545, Jan. 2016, doi: 10.1016/j.protcy.2016.05.094.
[8] M. Al-Shabi, "Simulation and implementation of real-time vision-based control system for 2-DoF robotic arm using PID with hardware-in-the-loop," *Intell. Control Autom.*, vol. 6, no. 2, pp. 147–157, 2015, doi: 10.4236/ica.2015.62015.
[9] L. Capito, P. Proaño, O. Camacho, A. Rosales, and G. Scaglia, "Experimental comparison of control strategies for trajectory tracking for mobile robots," *Int. J. Autom. Control*, vol. 10, no. 3, p. 308, 2016, doi: 10.1504/ijaac.2016.077591.

[10] L. Montoya-Villegas, J. Moreno-Valenzuela, and R. Pérez-Alcocer, "A feedback linearization-based motion controller for a UWMR with experimental evaluations," *Robotica*, vol. 37, no. 6, pp. 1073–1089, Jan. 2019, doi: 10.1017/s0263574718001443.
[11] L. Morales, M. Herrera, O. Camacho, P. Leica, and J. Aguilar, "LAMDA control approaches applied to trajectory tracking for mobile robots," *IEEE Access*, vol. 9, pp. 37179–37195, 2021, doi: 10.1109/ACCESS.2021.3062202.
[12] J. Borenstein, H. R. Everett, L. Feng, and D. Wehe, "Mobile robot positioning: Sensors and techniques," *J. Robot. Syst.*, vol. 14, no. 4, pp. 231–249, Apr. 1997, doi: 10.1002/(sici)1097-4563(199704)14:4<231:aid-rob2>3.0.co.2-r.
[13] W. Sakpere, M. A. Oshin, and N. B. Mlitwa, "A state-of-the-art survey of indoor positioning and navigation systems and technologies," *South Afr. Comput. J.*, vol. 29, no. 3, pp. 145–197, Dec. 2017, doi: 10.18489/sacj.v29i3.452.
[14] M. Dobrzanska and P. Dobrzanski, "Automatic correction of an automated guided vehicle's course using measurements from a laser rangefinder," *Appl. Sci.*, vol. 12, no. 24, p. 12826, Dec. 14, 2022, doi: 10.3390/app122412826.
[15] X. Zhang, Y. Fang, and N. Sun, "Visual servoing of mobile robots for posture stabilization: From theory to experiments," *Int. J. Robust Nonlinear Control*, vol. 25, no. 1, pp. 1–15, Aug. 2013, doi: 10.1002/rnc.3067.
[16] C. Pati and R. Kala, "Vision-based robot following using PID control," *Technologies*, vol. 5, no. 2, p. 34, Jun. 2017, doi: 10.3390/technologies5020034.
[17] M. O. A. Aqel, M. H. Marhaban, M. I. Saripan, and N. B. Ismail, "Review of visual odometry: Types, approaches, challenges, and applications," *SpringerPlus*, vol. 5, no. 1, pp. 1–26, Oct. 2016, doi: 10.1186/s40064-016-3573-7.
[18] T. D'Orazio, M. Ianigro, E. Stella, F. P. Lovergine, and A. Distante, "Mobile robot navigation by multi-sensory integration," in *Proc. IEEE Int. Conf. Robot. Autom.*, May 1993, pp. 373–379, doi: 10.1109/ROBOT.1993.292173.
[19] F. Hmeyda and F. Bouani, "Camera-based autonomous mobile robot path planning and trajectory tracking using PSO algorithm and PID controller," in *Proc. Int. Conf. Control, Autom. Diagnosis (ICCAD)*, Jan. 2017, pp. 203–208, doi: 10.1109/CADIAG.2017.8075657.
[20] R. Farkh and K. Aljaloud, "Vision navigation based PID control for line tracking robot," *Intell. Automat. Soft Comput.*, vol. 35, no. 1, pp. 901–911, 2023, doi: 10.32604/iasc.2023.027614M.
[21] M. Demirhan and C. Premachandra, "Development of an automated camera-based drone landing system," *IEEE Access*, vol. 8, pp. 202111–202121, 2020, doi: 10.1109/ACCESS.2020.3034948.
[22] C. Premachandra, D. N. H. Thanh, T. Kimura, and H. Kawanaka, "A study on hovering control of small aerial robot by sensing existing floor features," *IEEE/CAA J. Autom. Sinica*, vol. 7, no. 4, pp. 1016–1025, Jul. 2020, doi: 10.1109/JAS.2020.1003240.
[23] A. Cumani, "Feature localization refinement for improved visual odometry accuracy," *Int. J. Circuits Syst. Signal Process.*, vol. 5, no. 2, pp. 151–158, 2011.
[24] A. Cumani and A. Guiducci, "Fast stereo-based visual odometry for rover navigation," *Trans. Circuits Syst.*, vol. 7, pp. 648–657, Jul. 2008.
[25] N. Nourani-Vatani, J. Roberts, and M. V. Srinivasan, "Practical visual odometry for car-like vehicles," in *Proc. IEEE Int. Conf. Robot. Autom.*, May 2009, pp. 3551–3557, doi: 10.1109/ROBOT.2009.5152403.
[26] C. Patruno, R. Marani, M. Nitti, T. D'Orazio, and E. Stella, "Design of a low-cost vision system for laser profilometry aiding smart vehicles movement," in *Intelligent Autonomous Systems*. Cham, Switzerland: Springer, Sep. 2015, pp. 17–27, doi: 10.1007/978-3-319-08338-4_2.
[27] C. Patruno, R. Marani, M. Nitti, T. D'Orazio, and E. Stella, "Laser profilometry aiding smart vehicle control," *Int. J. Smart Sens. Intell. Syst.*, vol. 7, no. 5, pp. 1–6, Jan. 2014, doi: 10.21307/ijssis-2019-055.
[28] C. Patruno, R. Marani, M. Nitti, T. D'Orazio, and E. Stella, "An embedded vision system for real-time autonomous localization using laser profilometry," *IEEE Trans. Intell. Transp. Syst.*, vol. 16, no. 6, pp. 3482–3495, Dec. 2015, doi: 10.1109/TITS.2015.2459721.
[29] M. Adrian and G. Constantin, "PID controller based on a gyroscope sensor for an omnidirectional mobile platform," *Proc. Manuf. Syst.*, vol. 15, no. 1, pp. 27–34, 2020.
[30] R. Havangi, "Mobile robot localization based on PSO estimator," *Asian J. Control*, vol. 21, no. 4, pp. 2167–2178, Feb. 2019, doi: 10.1002/asjc.2004.
[31] O. A. Aguirre-Castro, E. Inzunza-González, E. E. García-Guerrero, E. Tlelo-Cuautle, O. R. López-Bonilla, J. E. Olguín-Tiznado, and J. R. Cárdenas-Valdez, "Design and construction of an ROV for underwater exploration," *Sensors*, vol. 19, no. 24, p. 5387, Dec. 2019, doi: 10.3390/s19245387.
[32] B. Mishra and A. Kertesz, "The use of MQTT in M2M and IoT systems: A survey," *IEEE Access*, vol. 8, pp. 201071–201086, 2020, doi: 10.1109/ACCESS.2020.3035849.
[33] I. Diddeniya, I. Wanniarachchi, H. Gunasinghe, C. Premachandra, and H. Kawanaka, "Human–robot communication system for an isolated environment," *IEEE Access*, vol. 10, pp. 63258–63269, 2022, doi: 10.1109/ACCESS.2022.3183110.
[34] M. I. Yamin, S. Kuswadi, and S. Sukaridhoto, "Real performance evaluation on MQTT and COAP protocol in ubiquitous network robot platform (UNRPF) for disaster multi-robot communication," *EMITTER Int. J. Eng. Technol.*, vol. 6, no. 2, pp. 369–385, Dec. 2018, doi: 10.24003/emitter.v6i2.305.

R. KARTHIK received the master's degree from Anna University, India, and the Ph.D. degree from the Vellore Institute of Technology, Chennai, India. Currently, he is an Associate Professor with the Research Centre for Cyber Physical Systems, Vellore Institute of Technology. He has published around 75 papers in peer-reviewed journals and conferences. His research interests include deep learning, computer vision, digital image processing, and medical image analysis. He is an Active Reviewer of journals published by Elsevier, IEEE, Springer, and Nature.

R. MENAKA received the master's degree in applied electronics and the Ph.D. degree from Anna University, Chennai, India. She is currently a Professor with the Centre for Cyber Physical Systems, Vellore Institute of Technology, Chennai. She has published around 80 papers in peer-reviewed journals and conferences. Her research interests include biomedical image and signal processing, neural networks, and fuzzy logic.

P. KISHORE is currently pursuing the Bachelor of Technology degree with the Vellore Institute of Technology, specializing in electronics and communication. His research interests include robotics, computer vision, AI, and deep learning.

R. ASWIN is currently pursuing the Bachelor of Technology degree with the Vellore Institute of Technology, specializing in electronics and communication. His research interests include robotics, computer vision, AI, and deep learning.

CHARAN VIKRAM is currently pursuing the Bachelor of Technology degree with the Vellore Institute of Technology, specializing in electronics and communication. His research interests include robotics, computer vision, AI, and deep learning.